Electronic Supplementary Material (ESI) for Polymer Chemistry.

Tailoring degradation and mechanical properties of poly(ε-caprolactone) incorporating functional ε-caprolactone-based copolymers

Mi Xu, Cuili Guo, Haozhen Dou, Yi Zuo, Yawei Sun, Jinli Zhang and Wei Li *

School of Chemical Engineering & Technology, Tianjin University; Collaborative Innovation Center of Chemical Science & Chemical Engineering (Tianjin), 300350, P. R. China

*Corresponding author at: School of Chemical Engineering & Technology, Tianjin University, Tianjin 300350, P.R.China. Tel: +86-22-27404495, Fax: +86-22-27403389.

E-mail address: liwei@tju.edu.cn

Contents

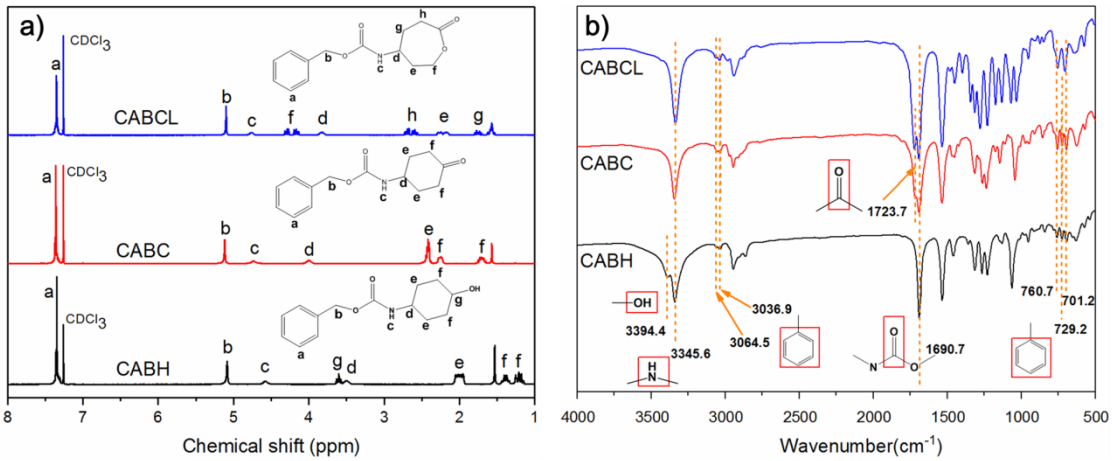

Fig. S1. ^{1}H NMR (a) and FTIR (b) spectra of CABH, CABC and CABCL.

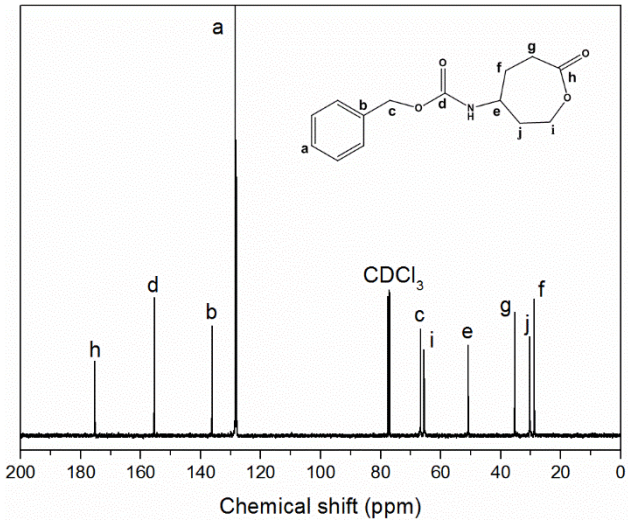

Fig. S2. ^{13}C NMR of CABCL.

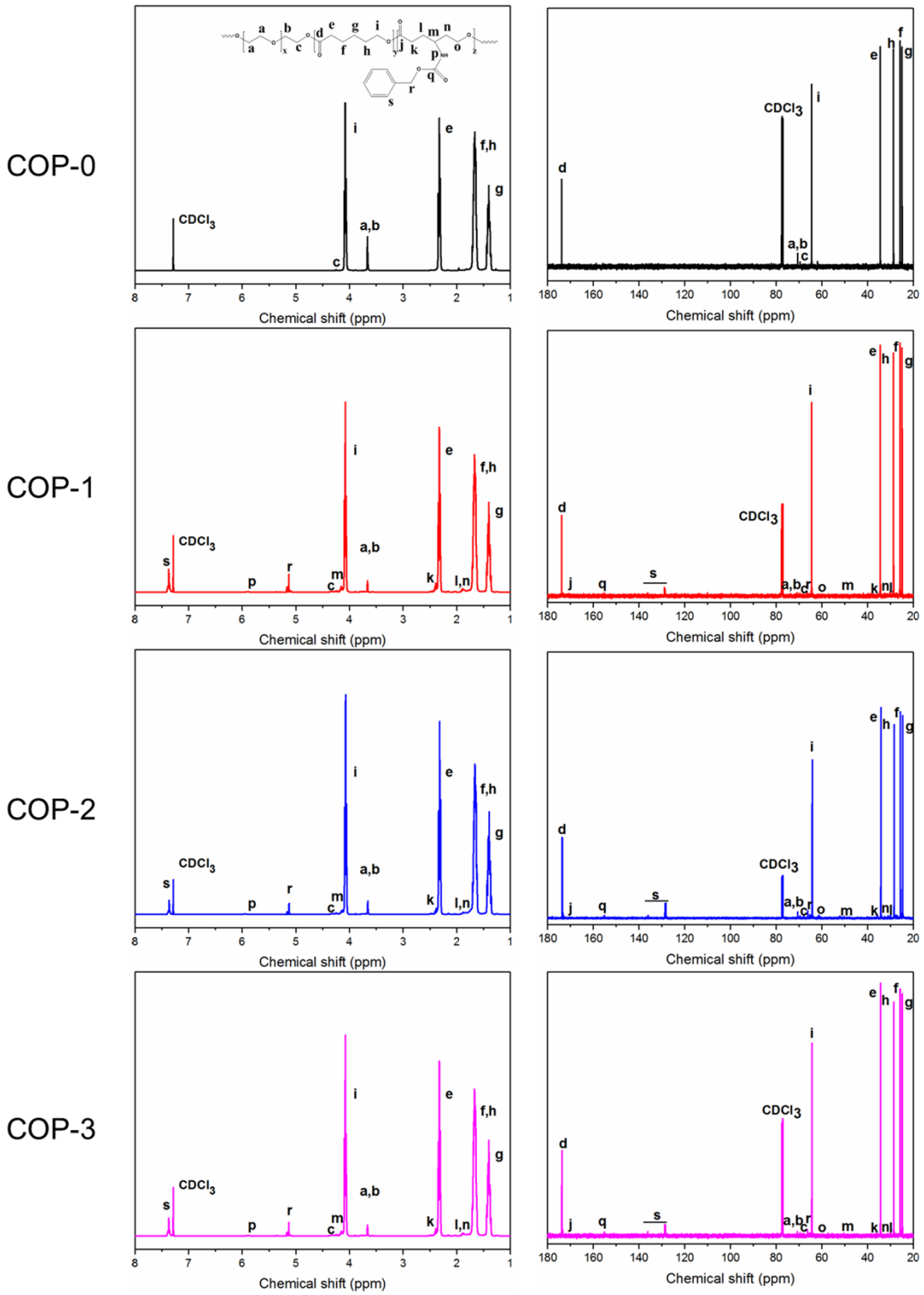

Fig. S3. ^{1}H NMR (left) and ^{13}C NMR (right) spectra of COP-0, COP-1, COP-2 and COP-3.

Table S1. Molecular weight (Mn) and PDI of the prepared COPs.

samples	Molar ratio of CABCL to CL	Mn (Da)	PDI
COP-0	0	10593	1.66
COP-1	0.033	8998	1.63
COP-2	0.05	6420	1.51
COP-3	0.1	5106	1.48

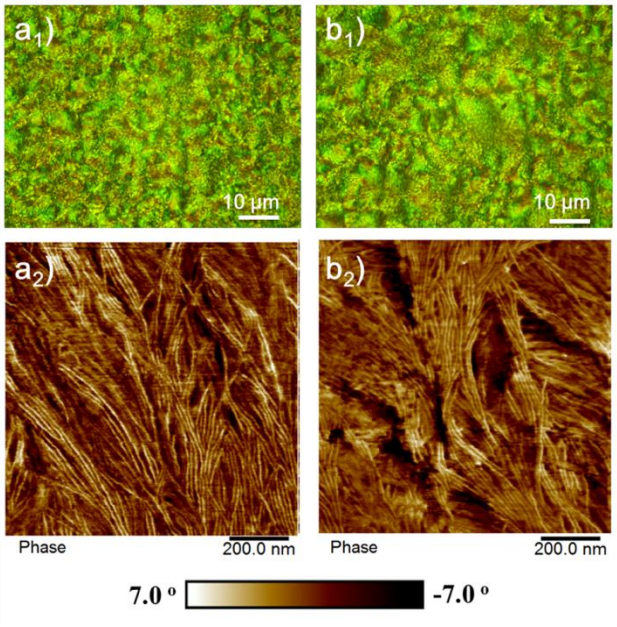

Fig. S4. Photographs (with the subscript of 1) and AFM phase images (with the subscript of 2) of film samples including (a) PCL/COP-1 and (b) PCL/COP-3.

Table S2. The long period (L) and the thickness of crystalline lamellae (L_c) of the film samples.

samples	q (nm^{-1})	L (nm)	L_c (nm)
PCL	0.36	17.62	9.37
PCL/COP-0	0.37	16.85	7.22
PCL/COP-1	0.40	15.75	8.60
PCL/COP-2	0.40	15.75	9.17
PCL/COP-3	0.40	15.75	8.98

Table S3. Crystalline characteristic parameters obtained by XRD.

samples	hkl	2θ (°)	d-space(Å)
PCL	110	21.399	4.1490
	111	21.984	4.0398
	200	23.722	3.7477
PCL/COP-0	110	21.416	4.1457
	111	22.018	4.0337
	200	23.672	3.7555
PCL/COP-1	110	21.416	4.1457
	111	22.001	4.0368
	200	23.771	3.7400
PCL/COP-2	110	21.432	4.1426
	111	22.100	4.0188
	200	23.772	3.7399
PCL/COP-3	110	21.415	4.1458
	111	21.985	4.0397
	200	23.738	3.7451

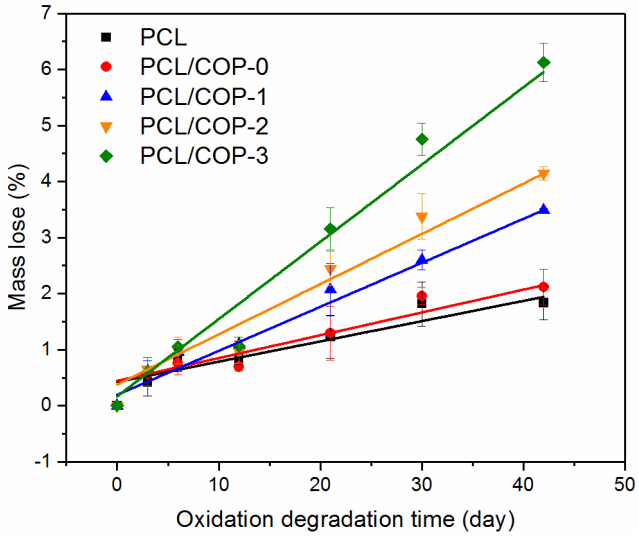

Fig. S5. The mass loss of the samples as a function of oxidative degradation time.

Table S4. The degradation rate constant of the samples after 42-day oxidative degradation.

samples	PCL	PCL/COP-0	PCL/COP-1	PCL/COP-2	PCL/COP-3
k (%/day)	0.036	0.041	0.079	0.090	0.138

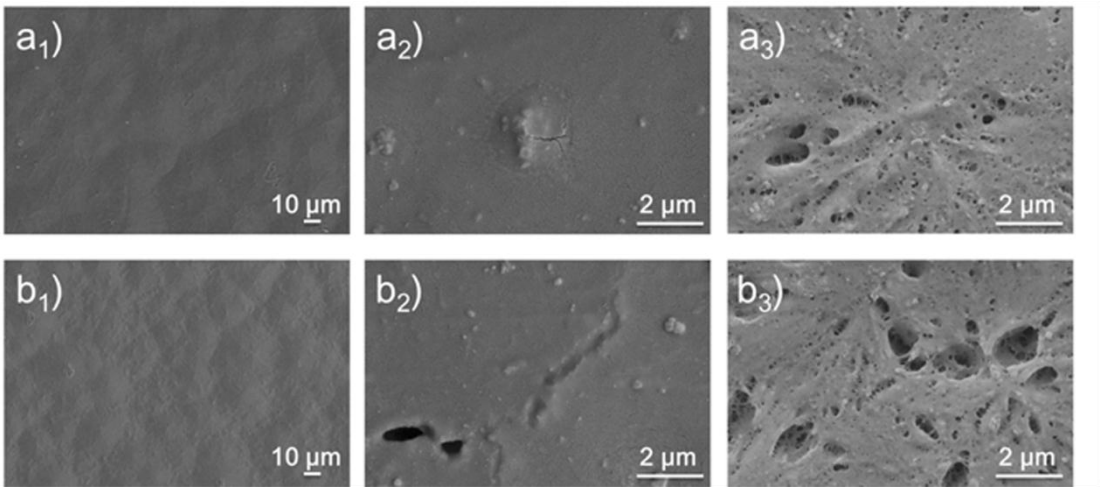

Fig. S6. SEM images of the original (with the subscript of 1), the 89-day hydrolysis-degraded (with the subscript of 2) and the 42-day oxidation-degraded (with the subscript of 3) samples of PCL/COP-1 (a) and PCL/COP-3 (b).

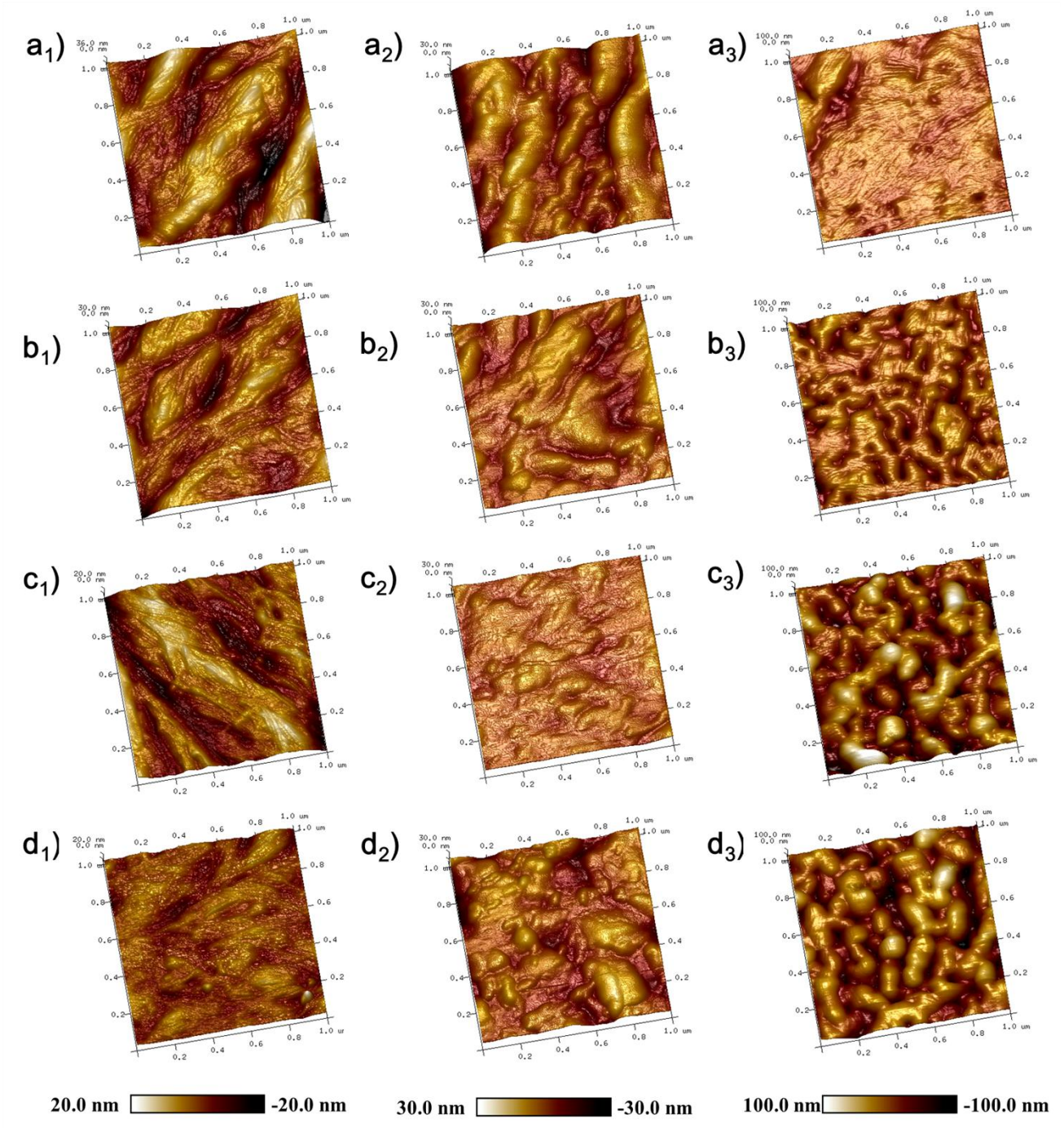

Fig. S7. AFM images of the original (with the subscript of 1), the 89-day hydrolysis-degraded (with the subscript of 2) and the 42-day oxidation-degraded (with the subscript of 3) samples of PCL (a), PCL/COP-0 (b), PCL/COP-1 (c) and PCL/COP-3 (d).

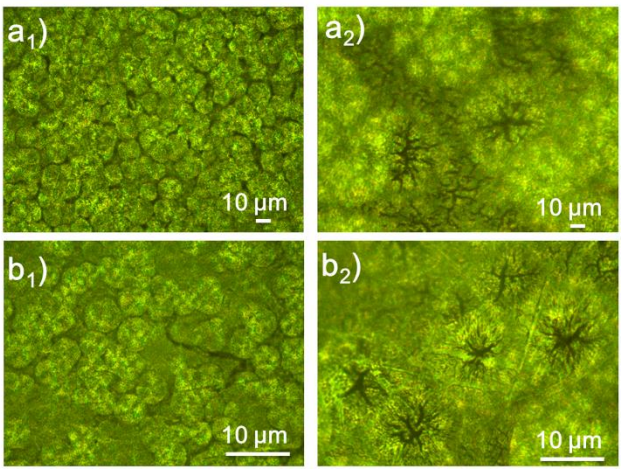

Fig. S8. POM images of the 89-day hydrolysis-degraded he original (with the subscript of 1) and the 42-day oxidation-degraded (with the subscript of 2) samples of PCL/COP-1(a) and PCL/COP-3(b).

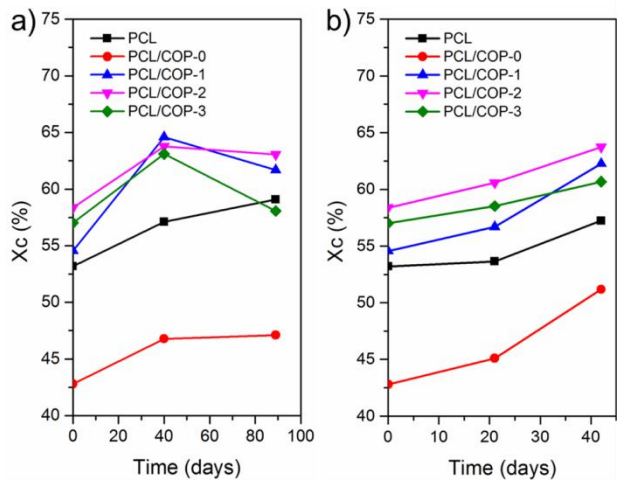

Fig. S9. Xc of samples during 89-day hydrolysis degradation (a) and 42-day oxidative degradation (b).

Experimental

Synthesis of CABCL

The CABCL monomer was synthesized through a three-step reaction process as shown in Fig. S15,[1] including 1) the preparation of benzyl 4-hydroxycyclohexane carbamate (CABH) using the raw materials of trans-4-aminocyclohexanol and CbzCl in the NaHCO3 aqueous solutions; 2) the preparation of benzyl 4-oxocyclohexane carbamate (CABC) via the oxidation of CABH; 3) the

preparation of CABCL through the reaction between CABC and m-CPBA in the solvent of CH_2Cl_2. The detailed steps are as follows.

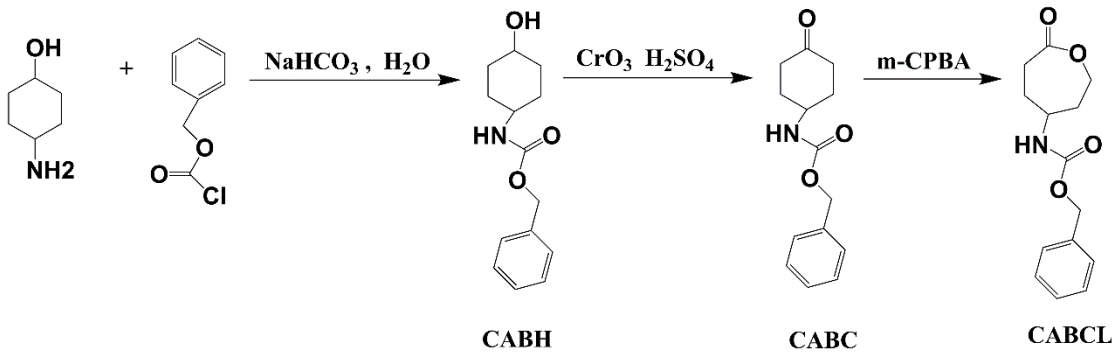

Fig. S10. The synthetic route of CABCL.

Synthesis of CABH

A 1000 ml four-necked flask was charged with a solution of trans-4-aminocyclohexanol (10.3 g) and $NaHCO_3$ (18.8 g) in 600 ml water, and the flask was placed in an ice water bath to be magnetically stirred to form a uniform solution. Then the CbzCl (20.09 g) was added dropwise and the process lasted for about 10 minutes. After that the temperature was slowly raised to 45 °C, and the reaction was carried out for 4 hours. The temperature was lowered to room temperature and the reaction lasted overnight. The reaction mixture was extracted with ethyl acetate and n-butanol, and the combined organic phases were washed three times with 0.5 M HCl, saturated $NaHCO_3$ solution and saturated NaCl solution successively, dried over anhydrous Na_2SO_4 and filtered. After spin steaming until CABH began to crystallize, the product was recrystallized in a refrigerator overnight to obtain white needle-like crystals, which were filtered and dried at 45 °C to a constant weight (yield 81%).

Synthesis of CABC

12 g of CABH and 172 ml of acetone were added to a 250 ml four-necked flask, and the flask was magnetically stirred in an ice water bath to form a uniform dispersion, and then 14 ml of Jones reagent was added dropwise for about 30 minutes. Then the reaction mixture was heated slowly to room temperature and stirred overnight. Thereafter, 3.5 ml of isopropanol was added to react with an excess of Jones reagent. After stirring for 1 hour, it was filtered and the mixture was steamed. The product was dissolved in 100 ml water and about 10 ml of a saturated $NaHCO_3$ solution was added to adjust the pH to neutral. The orange aqueous mixture was extracted with ethyl acetate and the organic phases

were combined and washed three times with saturated NaCl solution, and then dried over anhydrous Na_2SO_4, filtered, concentrated and recrystallized in ethyl ether and hexane (1:1) to afford the white crystalline solid. The solid was filtered and dried to constant weight (yield: 73%).

Synthesis of CABCL

A solution of CABC (6.0 g) in 25 ml of CH_2Cl_2 was added to a 250 ml three-necked flask and stirred magnetically. The three-necked flask was placed in an ice water bath, and m-CPBA (5.42 g) in CH_2Cl_2 (80 ml) was added dropwise. The addition was continued for about 30 minutes and then slowly warmed to room temperature and stirred overnight. The reaction solution was then washed three times successively with saturated $Na_2S_2O_3$ solution, saturated $NaHCO_3$ solution and saturated NaCl solution. The organic phase product was dried using anhydrous sodium sulfate overnight, followed by filtration, rotary evaporation, recrystallization using ethyl acetate/petroleum ether (3:2, v/v) and dry toluene (three times) and then dessication to obtain white needle crystals of CABCL, of which the purity was measured to be higher than 99.2% (yield 68%).

Characterization

Nuclear Magnetic Resonance Spectroscopy (NMR)

^1H NMR and ^{13}C NMR spectra were recorded on a Bruker Avance 500 (500 MHz) spectrometer with deuterated chloroform ($CDCl_3$) as the solvent and tetramethylsilane (TMS) as an internal standard.

Fourier Transform Infrared Spectrometry (FTIR)

FTIR spectra were recorded on a Nicolet iZ10 spectrometer in the range of 4000-500 cm^{-1} at a resolution of 4 cm^{-1} with 32 scans. The solid sample was mixed with dry KBr and pressed into a pellet, while the polymer sample was dissolved in CH_2Cl_2, and a film was cast on a piece of glass by evaporation of the solvent.

Gel Permeation Chromatography (GPC)

The molecular weights and polydispersity index (PDI) of the COPs were determined by gel permeation chromatography (GPC) using a Waters GPC system equipped with a Waters 1525 pump, a Waters 2414 refractive index detector, and a series of linear Styragel HT2, HT3 and HT4 columns, which was calibrated with a narrow molecular weight distribution polystyrene standard. Tetrahydrofuran (THF) was chosen as an eluent at a flow rate of 1.0 mL/min at 35 ^oC and the sample concentration in THF was 5-10 mg/mL.

Differential Scanning Calorimetry (DSC)

The thermal properties of neat PCL and PCL/COP samples were acquired with differential scanning calorimetry (DSC, Q2000, Waters China Ltd., American TA Company) by heating the sample (5~10 mg) in the sealed aluminum pans from -90 to 100 ℃ at a heating rate of 5 ℃/min in N_2 atmosphere.

Simultaneous Wide-Angle and Small-Angle X-ray Scattering (WAXD/SAXS)

The crystalline structures of the samples were examined with D/max-2500/PC diffractometer using a Cu Kα radiation (λ = 1.5418 Å) under a potential of 40 kV and a current of 100 mA. The 2D scattering patterns were carried out on a XEUSS SAXS/WAXS system. SAXS was performed in the scanning range of 0.5 º to 5 º with the rate of 0.5 º/min.

WAXD was performed from 10 º to 45 º on the 2θ scale at the scanning rate of 2.0 º/min and a step size of 0.02 º and WAXD curves were collected from the 2D-WAXD patterns. The d-spacing of a successive atomic plane was calculated by the Bragg equation.

$$2d\sin\theta = n\lambda$$

where θ is determined from XRD patterns, n is the diffraction order which adopting 1.

Scanning Electron Microscopy (SEM)

The surface morphologies of the samples were investigated by field-emission scanning electron microscope (SEM, Hitachi S-4800) at the accelerating voltage of 10 kV. For the samples experienced degradation, it needed washing and dessication before the routine measurement of SEM images.

Polarized Optical Microscope (POM)

The crystalline morphology of samples was observed using a polarizing microscope (POM, Sunny Optical Technology XY-P) with a CCD (YESONE, CS080) video camera.

Atomic Force Microscopy (AFM)

The surface morphology and roughness of the samples before and after degradation were investigated by AFM (Multimode 8, Bruker, Germany) using taping model with a drive frequency and scan rate at 300 kHz and 1 Hz, respectively. Phosphorus doped Si tips (RTESP) were purchased from Veeco with tip radius ranged from 8 nm to 12 nm. All the images were analyzed by Nanoscope image processing software and the root mean square surface roughness (Rq) was determined on the surface area of 1×1 μm^2.

Structural characterization of CABCL

The chemical structures of CABH, CABC and CABCL were characterized by the ^{1}H NMR and FTIR spectra, which have provided the evidence of their successful synthesis. As shown in Fig. S1, for all the three chemicals, the chemical shifts at 7.35 and 5.10 ppm were corresponded to the benzyl group (a) and methylene group (b), respectively, while the chemical shift at 4.76 ppm was were assigned to amine group (c). However, the ^{1}H NMR spectra also distinguished the chemical structure differences among three chemicals. As the hydroxyl group (CABH) was oxidized to carbonyl group (CABC), the chemical shifts of methylene groups (f) shifted to down-field. When the carbonyl group (CABC) was converted the corresponding ester group (CABCL), the chemical shifts of methylene groups (f, h) adjacent to ester group exhibited further down-filed, which located at the 4.17 and 2.67 ppm, respectively. The chemical structure of CABCL was also confirmed by ^{13}C NMR spectra (Fig. S2), which exhibited the characteristic peaks of amide, carbonyl and ester groups.

The FTIR spectra of three chemicals were also consistent with the desired structure. As shown in the Fig. S1b, the two marrow and weak peaks at 3064.5 and 3036.9 cm^{-1} were nominated as the aromatic C-H stretching vibration, while the peaks between 761~701 cm^{-1} attributed to aromatic C-H bending vibration, which are in good agreement with the previous study [7]. The stretching vibrations of N-H and C=O of amide group appeared at 3345.6 cm^{-1} and 1690.7 cm^{-1}, respectively. As for the FTIR spectrum of CABH, the stretching vibration of hydroxyl group appeared at 3394.4 cm^{-1}. Furthermore, the peaks at 1720.2 and 1723.7 cm^{-1} were corresponded to the carbonyl group of CABC and CABCL, respectively.

Reference

1. J. Yan, Y. Zhang, Y. Xiao, Y. Zhang and M. Lang, *Reactive & Functional Polymers*, 2010, **70**, 400-407.
2. J. E. Mark, *Polymer data handbook*, Oxford University Press, 1999.
3. J. K. Palacios, A. Tercjak, G. Liu, D. Wang, J. Zhao, N. Hadjichristidis and A. J. Müller, *Macromolecules*, 2017, **50**, 7268-7281.
4. Q. Zhang, W. Hua, Q. Ren and J. Feng, *Macromolecules*, 2016, **49**, 7379-7386.
5. L. Alexander, *X-ray diffraction methods in polymer science*, John Wiley & Sons,Inc, 1969.
6. Q. Zhang, L. Li, F. Su, Y. Ji, S. Ali, H. Zhao, L. Meng and L. Li, *Macromolecules*, 2018.
7. J. Yan, Z. Yi, X. Yan, Z. Yan and M. Lang, *Reactive & Functional Polymers*, 2010, **70**, 400-407.
8. L. Yang, J. Li, S. Meng, Y. Jin, J. Zhang, M. Li, J. Guo and Z. Gu, *Polymer*, 2014, **55**, 5111-5124.